DETECTION OF METABOLITES BY PROTON *EX VIVO* NMR, *IN VIVO* MR SPECTROSCOPY PEAKS AND TISSUE CONTENT ANALYSIS: BIOCHEMICAL-MAGNETIC RESONANCE CORRELATION: PRELIMINARY RESULTS

Rakesh Sharma*[1,2],Madan Rehani[1],Arun Agrawala[2]

[1]Department of Medical Physics, All India Institute of Medical Sciences,

[2]Department of Instrument Engineering (IDDC), Indian Institute of Technology,

New Delhi, ND 110029

ABSTRACT

Aim: Metabolite concentrations by in vivo magnetic resonance spectroscopy and ex vivo NMR spectroscopy were compared with excised normal human tissue relaxation times and tissue homogenate contents.

Hypothesis: Biochemical analysis combined with NMR and MR spectroscopy defines better tissue analysis.

Materials and Methods: Metabolites were measured using peak area, amplitude and molecular weights of metabolites in the reference solutions. In normal brain and heart autopsy, muscle and liver biopsy tissue ex vivo NMR peaks and spin-lattice (T1) and spin-spin (T2) relaxation times, were compared with diseased tissue NMR data in meningioma brain, myocardial infarct heart, duchene-muscular-dystrophy muscle and diffused-liver-injury liver after respective in vivo proton MR spectroscopy was done. NMR data was compared with tissue homogenate contents and serum levels of biochemical parameters.

Corresponding Author: Rakesh Sharma, Ph.D. Department of Medicine, College of Physicians and Surgeons, Columbia University, 630, West 168th Street, New York, NY 10032. Email: rs2010@columbia.edu

Results: The quantitation of smaller NMR visible metabolites was feasible for both ex vivo NMR and in vivo MR spectroscopy. Ex vivo H-1 NMR and in vivo MRS metabolite characteristic peaks (disease/normal data represented as fold change), T1 and T2, and metabolites in tissue homogenate and serum indicated muscle fibrosis in DMD, cardiac energy depletion in MI heart, neuronal dysfunction in meningioma brain and carbohydrate-lipid metabolic crisis in DLI liver tissues.

Conclusion: This preliminary report highlights the biochemical-magnetic resonance correlation as basis of magnetic resonance spectroscopic imaging data interpretation of disease.

Key words: MRS Magnetic Resonance Spectroscopy, NMR Nuclear Magnetic Resonance, DMD Duchene Muscular Dystrophy, MI Myocardial Infarction, DLI Diffused liver Injury

INTRODUCTION

Nuclear Magnetic Resonance (NMR) techniques are now extensively utilized for imaging and spectroscopy of diseased organs in the human body (1, 2). After initial success of in vivo NMR metabolite quantification, attempts were made to detect NMR peaks and resonance assignments and ways of correlating the in vivo MR spectroscopy peaks with biochemical reactions in the disease to make clinical decisions. Enormous efforts have been made in last decade in the direction of high-field clinical magnets, fast 3D localization schemes and robust software for *in vivo* MR spectroscopy and ex vivo NMR studies aimed at measuring *in vivo* metabolite concentrations in tissues. In recent past, non-invasive NMR and in vivo metabolic characterization has attracted considerable attention of chemical NMR spectral characterization in clinical radiology. The potential of this non-invasive technique in providing detailed metabolite concentrations and metabolic screening in selective image area have not been fully explored. The reason of doubt on the complete success of this non-invasive tool is now realized due to insufficient information on the relaxation values, MR-visibility and reliable quantitation of metabolites by NMR and MRS methods. However, these clinical methods are in infancy and limited to research studies promising it of high value [1,2,3,4]. Both of them suffer from several factors such as spatial resolution, chemical shift resolution and peak assignments and their peak standardization is not yet resolved despite of several methods applied [4,5]. The potentials of this non-invasive technique in providing detailed metabolite concentrations and metabolic screening in selective image area have not been fully explored due to lack of sufficient information on the MR-visibility of metabolites by NMR and MRS methods. Quantification of these metabolites suffers from several factors and method is not yet resolved. Main reasons for this discrepancy are incomplete information on the in vivo dynamic patho-chemical changes in tissues and their effects on NMR and physical parameters of diseased tissues [6]. The obvious reason of it is complexity of in vivo

NMR signal as outcome of physical, chemical and biological processes at the molecular level. It makes difficult the interpretation of observed NMR signal and its correlation with metabolic component in the tissue. Still, ideal most approaches of in vivo MR spectroscopy and correlative biochemical analysis of disease (metabolic screening) to make accurate, specific clinical decision are far from clinical acceptability. However, it indicated that *in vitro* NMR information of tissue can be extrapolated to *in vivo* tissue processes [7, 8]. Various NMR in vitro and in vivo spectroscopy techniques can predict both qualitative and relative quantitative information on biochemical contents in tissues. The possibility of non-invasive clinical MR spectroscopy measurements opened new vistas for NMR methods to become diagnostic tool [7, 8, 9]. Moreover, there is paucity of information in literature on identification and quantification of MR 'visible' metabolite peaks by in vitro and in vivo H-1 NMR spectroscopy of normal and diseased tissues like normal liver, muscle, heart and brain.

The present study, we focused on measurements of T1 and T2 relaxation values, identification and quantitation of metabolites by ex vivo NMR resonances and comparison with in vivo MR visible peaks and tissue homogenate contents as NMR specific tissue characteristics. It is a preliminary attempt also to analyze *in vivo* MR visible metabolites and compare them with *a priori knowledge* based high resolution *ex vivo* NMR visible metabolites in perchloric acid tissue extracts. For it, model metabolite solutions were analyzed for their high resolution *in vitro* NMR chemical shift peak positions. Duchene Muscular Dystrophy (DMD) muscle and diffused liver injury(DLI) liver (right lobe) biopsies and meningioma (MB) brain (cerebrum), myocardial infarction(MI) heart(left ventricle) autopsy tissues extracts were compared with tissue extracts from normal tissues for T1, T2 relaxation constants and tissue biochemical contents in patient sera. The comparison of serum biomarkers and tissue contents with tissue MR information may be useful to interpret laboratory data and *in vivo/ex vivo* MR data correlation. Taking together NMR visible metabolites and tissue homogenate contents along with altered serum clinical chemistry values it is possible to predict better biochemical definition of the organ specific diseases.

Materials and Methods

The excised tissue longitudinal (T1) and transverse (T2) relaxation constants were measured using Bruker Biospec NMR spectrometer at 90 MHz magnetic field by inversion recovery and Carr-Purcell McGill (CPMG) methods respectively [9].

For *in vivo* MRS localized and *ex vivo* H-1 NMR spectroscopy, patients with proven history of Duchene Muscular Dystrophy (DMD), myocardial infarction(MI), meningioma(BM) and diffused-liver-injury (DLI), were recruited to get liver and muscle

biopsies and heart and brain autopsies as recommended by institutional human research ethical committee at institute hospital. The selection of patients and specimen collection was in compliance with purpose to include documented acute episode of these diseases and minimal injury during study. For other tissue experiments of *ex vivo* NMR and tissue content analysis, Duchene Muscular Dystrophy (DMD) muscle and diffused liver injury(DLI) liver(right lobe) biopsies and meningioma(MB) brain(cerebrum), myocardial infarction(MI) heart(left ventricle) autopsies were obtained as by-products from operation theatre. These tissues were frozen in liquid N_2 and each tissue was used for tissue homogenate preparation by sonication process at 4°C for 3 minutes for liver and brain, and 20 minutes for muscle and heart specimens. These homogenates were used for measurement of lipids, pyruvate and lactate and patient sera were used for enzymes alkaline phosphatase, SGPT, SGOT, creatine kinase, pyruvate and lactate assay on clinical chemistry analyzer [10]. Simultaneously, *in vivo* MRS and *in vitro* NMR biopsy spectra peaks were identified and compared to measure the metabolite concentrations.

In Vivo MR Spectroscopy

For *in vivo* MRS localized spectroscopy of DMD and MB patients were positioned supine under surface coil covering reference location by its axial and sagittal beams. The area of interest was positioned in axial plane to place it close with magnet isocenter. Shimming coils focused on water signal to selected area at carrier frequency.

For DMD, gastronemius muscle, spectra were recorded and metabolites were measured on a 1.5 Tesla MR unit with a H-1 double surface coil having an 8 inch transmitter and 3 inch receiver coil [11]. Selective water suppressed H-1 spectra were taken with 1331 pulse-depth resolved surface coil spectroscopy program at following setting: spectral width 650 MHz, TR = 3000 ms, TE = 25 ms, data points = 1024; inter pulse variation =2.5 – 3.0 ms [12]. Base line correction, resolution enhancement, manual FT-spectral phasing were made. The 1331-pulse sequence caused 180° phase shift between aliphatic and aromatic spectral regions (aliphatic peaks up and aromatic peaks inverted). Water suppression H-1 spectral chemical shifts were referenced to the position of water at 4.86 ppm [12, 13]. The metabolite peaks assignment and concentrations were measured by using NMR 1 and Peakfit software (SPSS, Korea).

For *in vivo* MRS localized spectroscopy of heart, patients were positioned under surface coil by sagittal beams. The resolution enhancement was made by multiplying FID free induction decay with sine function before Fourier transform and exponential filtering. Hahn spin echo pulse sequence was used to eliminate short T2 protons of cell by 60 ms delay

between 90 degree and 180 degree pulses. Scan settings were similar as above in muscle in vivo MRS [12, 13].

For *in vivo* MR localized spectroscopic studies were done on 5 patients suffered from meningioma. 1.5 Tesla MR unit was using head coil with circularly polarized B1 field using 3 slice selective 90° RF pulses creating stimulated echo, was used. Echoes from protons of 3 slices belonging to selective volumes were thus obtained. The interval of second and third slice selective RF pulse was kept 30 ms constantly with suitable variations of T1 and T2 weighting. Stimulated echo were obtained at completely relaxed water signal reference with following setting: data points = 4096; TR = 1000 ms; TE = 62 ms; spectral width = 4 Hz with base line correction, resolution enhancement, manual FT spectral phasing by phase correction with constant phase angle. The signal stemming from metabolites was obtained by the preceding sequence by three 90° chemical shifts selective pulses at Larmor frequency of water with bandwidth = 60 Hz. Water relaxed signal was taken as internal standard. Chemical shifts were referenced to the position of water (4.78 ppm) [2, 3, 4]. Proton resonances of spectra were assigned on the basis of standard assignments. Biochemical assays for lactate, pyruvate and acetoacetate were measured in homogenates and SGOT, lactate and pyruvate in sera by Boeringer Manheim kit methods [10].

For in vivo MRS of liver, patients were positioned under surface coil covering reference location by its axial and sagittal beams. Selective water suppressed 1H spectra were taken with 1331 pulse depth resolved surface coil spectroscopy program with scan setting at spectral width = 650 MHz, TR= 3000 ms, TE= 25 ms, data points=1024, inter pulse variation= 2.5 and 3.0 ms [15]. The 1331 pulse sequence caused 180 degree phase shift between aliphatic upside with chemical shift change 0.1 ppm and aromatic inverted spectra peaks.

Ex Vivo NMR Spectroscopy

For *ex vivo* NMR experiments, powder was prepared by 70 % perchloric acid treatment (0.1 ml/ml of tissue perfusate). The muscle was inserted into an NMR tube and minimum amount of isotonic D_2O in Ringer solution was added for NMR locking. For calibration, a capillary containing 10 % tetramethylsilane in $CDCl_3$ was inserted as external reference. H-1 NMR spectroscopy using selective water saturation technique was carried out on JEOL-400 FX PFT-400 MHz instrument located at central NMR facility [9]. Chemical shifts were referenced relative to $=N.CH_3$ of creatine assigned as δ=3.0(TSP in D_20 at 0.0 ppm). Hahn spin echo pulse sequence used to eliminate short T2 protons of cell, by 60 ms delay between 90° and 180° pulses. The field frequency was controlled by locking the deuterium signal of the H_2O solution added in the sample while the sample tube was spun at room temperature of

30°C. For selective water saturated NMR signals in the muscle sample, NMR probe circuit was modified to perform homonuclear gated proton decoupling. A time interval of 5 seconds was taken between the end of accumulation at each free induction decay and next analytical pulse. During this time interval, the water frequency was irradiated with sufficient power to saturate the signals of water proton. The irradiated power by tuning power amplification degrees of NMR transmitter was used and the value of 30 dB corresponded to several mG. H-1 NMR spectra were obtained by accumulation of 100 scans with Fourier transforms being performed every 10 scans of free induction decay obtained by a 90° pulse. The high resolution spectral portion was obtained by subtracting broad component from original spectra. Some spectra were measured by high resolution NMR spectroscopy where 90° -τ -90 °- τ, 1331 water suppression pulse sequences were used for D_2O extracts by one pulse sequence with pulse angle 90°, recycling time 1.7 seconds. Chemical shifts were referenced relative to $=N.CH_3$ of creatine assigned as $\delta = 3.0$ (referenced against to external TSP in D_2O at 0.0 ppm. Biochemical serum analysis for creatine kinase and SGPT was done by routine autoanalyzer methods [10].

Myocardial infarction heart autopsy samples were obtained from autopsy room. 50 grams pieces from ventricular heart were quickly frozen after they were perfused at 37 °C with oxygenated (90 % O_2 with 5 % CO_2) carbogen gas in Kreb's Hanseleit buffer (pH 7.4) as previously explained. The heart perchloric extracts were prepared as previously explained. Freeze dried powder dissolved in 99 % D_2O which was obtained by 70 % perchloric acid treatment (0.1 ml/ml tissue perfusate) and centrifugation at 2000 x g for 15 minutes at 4°C. The samples in D_2O were used for NMR mesasured [9]. Water presaturation pulse sequences were used for D_2O extracts followed by 90°-τ-180°-τ Hahn spin echo NMR pulse sequence. Multiplying FID with sine function before Fourier transform and exponential filtering made resolution enhancement. Chemical shifts were recorded with reference to TSP added to extracts. Hahn spin echo pulse sequence used to eliminate short T2 protons of cell, by 60 ms delay between 90° and 180° pulses(1). H-1 in vitro NMR and in vivo MRS were done using procedures similar to those for muscle studies. Biochemical estimations for creatine kinase-MB, cholesterol, triglycerides, SGOT and lactate made using standard procedure [10].

Brain autopsy samples were used for in vitro NMR spectroscopy. Brain tissues were immediately cooled in liquid nitrogen gas at 15 seconds and homogenized at 4 °C in Kreb's Henseleit buffer(pH 7.4) in D_2O using Potter Elvehjem homogenizer with teflon pestle and sonicated to 20 seconds at 3 °C to improve homogeneity. In vitro NMR spectra were recorded at 37 °C on pulsed Fourier transform mode using 180°-τ-90° inversion recovery spin echo IRSE pulse sequence with inter scan delay of 1 second, $\tau = 0.6$ seconds, TR = 2 seconds, data points = 8192, spectral width = 500 Hz. Resolution peaks were enhanced with Gaussian multiplication. Tetramethylsilane (TMS) was used as 0.0 ppm reference and was placed in

capillary within the NMR tube. Hahn spin echo pulse sequence used to eliminate short T_2 protons of cell, by 60 ms delay between 90° and 180° pulses [12].

Nine patients suffering from diffused liver injury were clinically investigated with need of *ex vivo* NMR spectroscopy information. Liver biopsy obtained from surgical operation theatre and extracts were prepared in the same manner as muscle biopsy samples were processed for *in vitro* NMR spectroscopy. The *in vitro* NMR measurement was made with selective water saturation technique. Selective spin echo sequence consisting 90° –180° at delay time 60 ms, 4096 data points, spectral bandwidth = 350 Hz against water reference at 4.76 ppm at 30 °C. Measurements were made using selective selection water suppressed H-1 spectra in Fourier transform mode using 180°-τ-90° inversion recovery spin echo IRSE pulse sequence [16]. Base line correlation, resolution enhancement, manual Fourier transform spectral phasing was done manually. This pulse sequence caused a 180° pulse shift between aliphatic and aromatic spectral regions (aliphatic peaks up and aromatic peaks inverted). All were phased up with chemical shift change 0.1 ppm [10].

For quantification of metabolites, concentration of metabolites was measured by robust automated quantification based upon formula:

$$\mathrm{Conc}(x) = \mathrm{conc}(X)\frac{MW(x).(\text{peak area}).(\text{peak amplitude}(x)).\text{peak width}(x)}{MW(X).(\text{peak area}).(\text{peak amplitude}(X)).\text{peak width}(X)}$$

where x is metabolite to be measured, X is reference metabolite and MW refers to molecular weight. Standard peak assignments and peak area measured the concentration of creatine, aspartate, choline, glutamate and other reference solutions.

The standard reference solutions were used for distinct NMR resonance assignments (see Figure 1 and Appendix 1) for following peaks:

NAA: A large singlet arises from three protons in methyl group. The resonances of three protons of –CH2 group and single proton of CH group are NMR visible as 12 resonances in this ABX spin system in the molecule.

Alanine: A quartet at 1.45 ppm and doublet at 3.8 ppm origeinate from CH and CH3 groups in NMR while single peak at 1.45 ppm in MR spectrum.

Choline: A very large resonance at 3.2 ppm due to 9 equivalent protons of three CH3 groups and tiny several resonances of two CH2 groups are NMR visible in choline molecule.

Myo-inositol: Six CH group protons of inositol ring show up a large singlet at 3.6 ppm and two resonances at 3.56 (C3 protons) and 4.06 ppm (C2 proton) by NMR spectrum while MR spectrum shows only one singlet at 3.6 ppm.

Glutamate and Glutamine: In NMR spectrum, glutamate symmetric molecule CH group and glutamine NH2 groups both show up as triplet peak at 3.75 ppm and complex multiplet tetrad peak from two CH2 groups (4 protons) at 2.1 to 2.4 ppm in NMR spectrum.

Creatine: In NMR spectrum, creatine -CH2- protons showed strong peak at 3.0 ppm and two other smaller peaks.

GABA: Three CH2 groups show up at three different peaks including 2.95 ppm as triplet, second triplet at 2.2 ppm and a quintet at 1.95 ppm as a result interactions between three CH2 groups as visible NMR peaks while MR spectrum shows only singlets at 1.9 and 2.2 ppm.

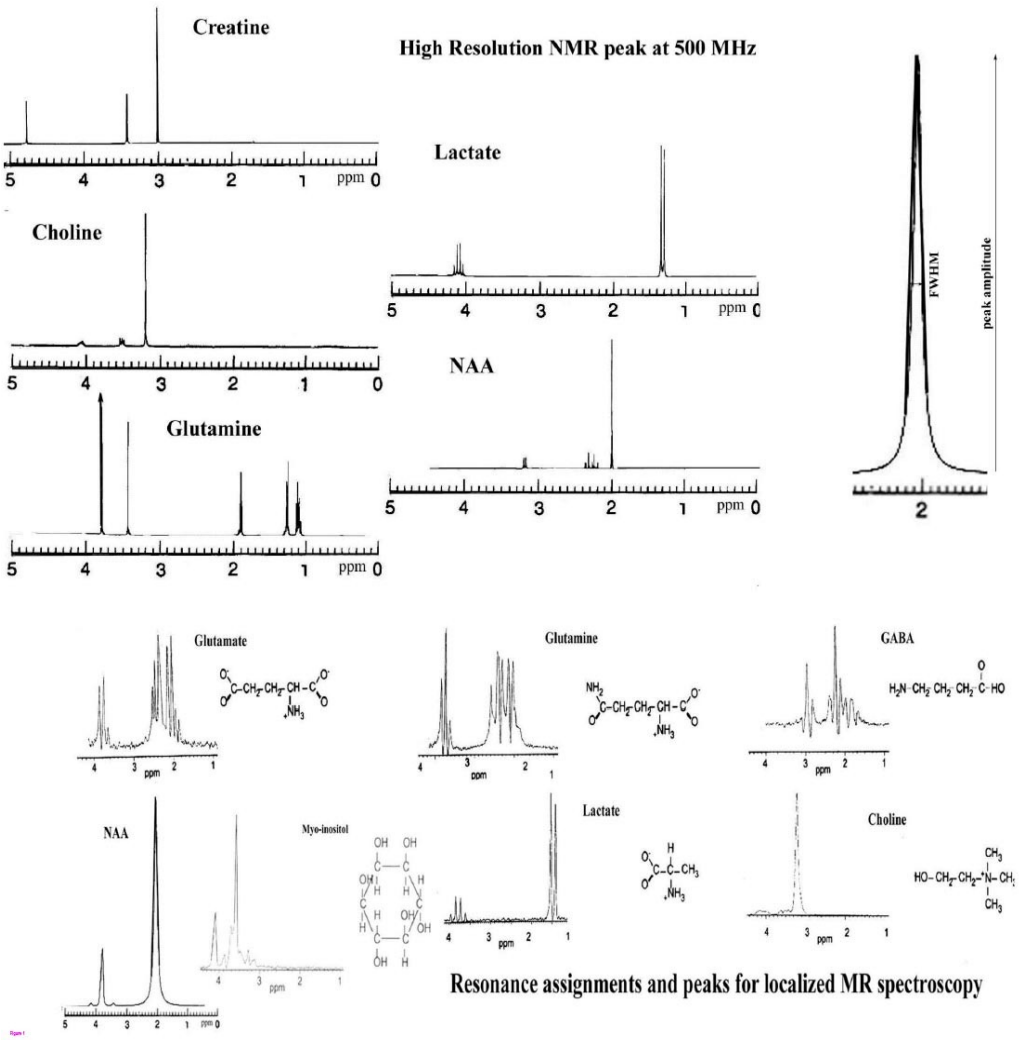

Figure 1. Ex vivo standard H-1 500 MHz NMR spectra of reference metabolites (creatine, choline, glutamine/glutamate, lactate, NAA, GABA, myo-inositol are shown with their peaks used to match

resonance assignments by ex vivo NMR and in vivo MR spectroscopy of tissues. For calculation of relaxation time, peak height at half width (FWHM) is shown on at top on right. The lower two rows show the high resolution NMR spectroscopy spectral assignments of molecules with their protons and structures.

For quantitation of metabolites we used micrometer method to measure peak area and comparison with peak area of reference solutions of known concentrations as shown in Figure 1. For relaxation times (T1 and T2) measurements of different normal and diseased tissues, 15 mm^3 tissue cubes were placed in 505 Wilmad NMR tube bottom and T1 (inversion recovery pulse sequence), T2 (CPMG pulse sequence) were measured with usable echo obtained every 10 ms [17].

RESULTS

Ex vivo H-1 NMR and in vivo MRS metabolite peaks, T1 and T2, tissue homogenate contents and serum metabolites in normal human tissues were compared with DMD muscle, MI heart, meningioma brain and DLI liver tissues (disease/normal data represented as fold change). The comparison of clinically relevant relaxation times T1 and T2, NMR/MRS, tissue contents and serum chemistry data are shown in different tissues as Tables 1-4.

Ex vivo NMR peaks (Figure 2) and in vivo MRS peaks (Figure 3) in different tissues are shown as curve-fitted spectra for peak-area measurement by NMR-1 program. For peak identification, different peaks were labeled to distinguish peaks in diseased tissues. Different spectral peaks were compared by NMR and MRS methods. Calculation method of metabolite concentrations by NMR and MRS methods was field independent. However, normal and diseased tissues showed distinct relaxation times.

Ex vivo H-1 NMR spectra of DMD muscle exhibited (see Figure 2 A) decreased lactate (18 fold), increased glutamine(1.5 fold); in vivo H-1 MRS peaks evidenced (see Figure 3 A) increased PCr (2-6 fold), fatty acids(12 fold) as a result of muscle fibrosis (Table 5). Furthermore, elongated relaxation times T1 (1.6 fold), T2 (1.3 fold); DMD muscle homogenate decreased phospholipids (0.49 fold), triglycerides (0.9 fold) levels and elevated serum SGPT (5 fold) and creatine kinase (2.6 fold) were observed.

Ex vivo H-1 NMR spectra of MI heart evidenced (see Figure 2 B) increased cholesterol (51.5 fold), taurine (2.8 fold), creatine (32.3 fold) with decreased PCr/Cr (0.54 fold); in vivo H-1 NMR peaks evidenced (see Figure 3 B) increased cholesterol (2.27 fold) and PCr/Cr (1.6 fold), T2 (1.16 fold), increased cholesterol (1.5 fold), lactate (1.5 fold) shown in Table 6. MI

heart autopsy homogenates showed elevated lactate (1.52 fold) and cholesterol (1.46 fold), elevated serum SGOT(6 fold), CK-MB(3.24 fold) and lactate(2.4 fold) were observed.

Ex vivo H-1 NMR spectra of meningioma brain evidenced (see Figure 4 A) increased lactate (1.32 fold), alanine (2.7 fold), creatine (2.1 fold) and decreased acetate (0.5 fold); in vivo H-1 NMR spectra evidenced (see Figure 4 B) increased aspartate (15.3 fold), decreased PCr/Cr (0.28 fold) as a result of displacement of neuronal cells by meningioma and energy depletion (Table 7). Further, elongated relaxation times T1(1.1 fold), T2 (1.6 fold); meningioma brain homogenate increased lactate(1.7 fold), decreased pyruvate(0.87 fold), acetoacetate (0.56 fold) levels and serum elevated levels of lactate(3.5 fold), SGOT(2.77 fold) and decreased pyruvate(0.83 fold) were observed.

Ex vivo H-1 NMR spectra of diffused liver injury effected liver (see Figure 5 A) showed increased PCr/Cr(2.2 fold), phosphorylcholine (8.5 fold), taurine (4 fold); in vivo H-1

NMR spectra evidenced (see Figure 5 B) decreased aspartate (0.43 fold), as a result of lipid and carbohydrate metabolic crisis (Table 8). Furthermore, elongated relaxation times T1 (2.09 fold), T2 (1.6 fold); DLI liver homogenates increased phospholipids (1.5 fold), triglyceride (1.5 fold) levels and serum elevated of SGPT (7.6 fold), alkaline phosphatase (6 fold) and bilirubin (2.8 fold) were observed.

Table 1. Comparative NMR-biochemical correlation analysis of muscle by different methods (n=7)

Method	Normal muscle	Duchene Muscular Dystrophy muscle
In vitro pulsed NMR		
T1	600±20 ms	1049±86 ms
T2	65±9 ms	98±4 ms
In vitro NMR spectroscopy		
Lactate	37.6 mM	2.3 mM
Glutamate	11.8 mM	19.5 mM
In vivo NMR spectroscopy		
Phospholipids	26 mM	106 mM
Fatty acids	29 mM	347 mM
Biochemical tissue metabolite contents(n=6)		
Phospholipids	139.7±12.4 mg %	68.8±8.3 mg%
Triglycerides	30.2±8.1 mg%	26.7+5.9 mg%
Biochemical serum levels* (n=7)		
Creatine kinase	21.1±2.9 IU	55±2.4 IU

SGPT	13.6±1.4 IU	69±10 IU

*IU is defined as µ moles substrate used per minute per mg enzyme protein.

Table 2. Comparative NMR-biochemical correlation analysis of old myocardial infracted-hypertensive heart by different methods (n=7)

Method	Normal heart autopsy	MI-hypertensive autopsy
In vitro pulsed NMR		
T1 ms	946±30 ms	1126±46 ms
T2 ms	68±9 ms	79±12 ms
In vitro NMR spectroscopy		
Cholesterol	0.74 mM	38.1 mM
Phosphocreatine*/creatine	18*±6.1 mM	6.3±6.3 mM
Taurine(total)	67.2*±16.8 mM	187.5*±51.9 mM
Creatine	0.20 mM	6.46 mM
In vivo NMR spectroscopy		
Cholesterol	13.5 mM	30.7 mM
Phosphocreatine/creatine	24.0 mM	38.1 mM
Biochemical tissue metabolite contents (n=6)		
Triglycerides	106±8.1 mg%	110±9.6 mg%
Cholesterol	175±5.8 mg%	256±21.3 mg%
Lactate	89.4±4.8 µg%	136.6±2.9 µg%
Biochemical serum levels** (n=7)		
SGOT	23.4±2.9 IU	142.5±34.5 IU
CK-MB	19.5±2.4 IU	63.2±3.1 IU
Lactate	24.8±7.9 µg%	69.2±16.5 µg%

*Phosphocreatine peak areas were used to calculate concentration.

**IU is defined as µ moles substrate used per minute per mg enzyme protein.

Table 3. Comparative NMR-biochemical correlation analysis brain with meningioma by different methods

Method	Normal brain	Meningioma
In vitro pulsed NMR:		
T1	774±23 ms	849±15.2 ms
T2	145±81 ms	234±16 ms
In vitro NMR spectroscopy		
Lactate	14.4 mM	19 mM
Alanine	0.79 mM	2.16 mM

Acetate	0.22 mM	0.11 mM
Creatine	2.61 mM	5.5 mM
In vivo NMR spectroscopy		
N-acetyl aspartate	18 mM	-
Glutamine/glutamine	7.2 mM	-
Aspartate	2.3 mM	35.3 mM
Phosphocreatine/creatine	72.3 mM	20.0 mM
Biochemical tissue metabolites (n=5)		
Lactate	146.6±8.8 µg%	249±4.8 µg%
Pyruvate	98.8±3.5 µg%	86.2±4.9 µg%
Acetoacetate	36.6±2.1 µg%	20.5±1.8 µg%
Biochemical serum levels* (n=5)		
Lactate	24.8 µg%	85.5 µg%
Pyruvate	95.6 µg%	79.8 µg%
SGOT	23.4 IU	64.8 µg%

*IU is defined as µ moles substrate used per minute per mg enzyme protein.

Table 4. Comparative NMR-biochemical correlation analysis of liver with diffused injury by different methods

Method	Normal liver	Diffused liver injury
In vitro pulsed NMR		
T1 ms	448±20 ms	939±11 ms
T2 ms	88±7 ms	144±9 ms
In vitro NMR spectroscopy		
Phosphocreatine/creatine	0.48 mM	1.06 mM
Phosphorylcholine	7.2 mM	61.3 mM
Taurine	5.75 mM	23 mM
In vivo NMR spectroscopy		
Glutamine	36.1 mM	35.2 mM
Aspartate	6.27 mM	2.7 mM
Biochemical tissue metabolites		
Phospholipids	113.8±3.9 mg%	168.9±5.6 mg%
Triglycerides	89.7±4.8 mg%	139.9±3.6 mg%
Biochemical serum levels*		
SGPT	18.5±1.9 IU	140.9±15.4 IU
Alkaline phosphatase	39.5±7.8 IU	239.9±23.4 IU
Bilirubin	1.5±0.2 mg%	4.2±0.6 mg%

*IU is defined as µ moles substrate used per minute per mg enzyme protein.

Table 5. I. Resonance assignment and quantification of lactate, glutamine, alanine metabolites in normal muscle (a); and Duchene muscular dystrophy (DMD) muscle (b)

in perchloric acid extracts by ex vivo H-1 NMR inversion recovery spectra as shown in Figure 1A. The NMR reference metabolite standard was 60 mM choline solution for metabolite concentration measurement

Chemical shifts (ppm)	assignment	Peak area*(mm^2) Normal muscle (a)	Concentration(mM) DMD muscle (b)
1.5	-(CH_2)n phospholipids	26(18.2)	106(51.5)
1.83	=$CH(CH_2)$-(linoleic acid)	6(6.5)	64(36.8)
2.11	=$CH(CH_2)$-(linolenic acid)	1(1.32)	62(21.6)
2.19	=$CH(CH_2)$-(Arachidonic acid)	9(4.62)	80(24.6)
2.42	=$CH(CH_2)_2$-(Arachidonic acid)	8	65
5.34	-CH=CH- of	3	18
5.4	Linolenic and	2	21
5.7	Arachidonic acids)	-	26
5.95		-	11
6.38		-	18

*signifies peak assignments with clinical significance.

II. Quantification of fat metabolites in normal (a) and Duchene muscular dystrophy (DMD) muscle (b) by in vivo MR spectroscopy peaks shown in Figure 2A. The NMR reference standard was 40 mM glutamate solution for metabolite concentration measurement

Chemical shift (ppm)	Resonance assignment	Peak area (mm^2)		Concentration (mM)	
		Normal (a)	DMD (b)	Normal (a)	DMD (b)
1.3	-CH_3 lactate	28	19	37.6	2.3
4.1	-CHOH lactate	2	2	-	-
2.12	C H $_2$ glutamine	15	26	11.8	19.5
2.43	C H $_2$	2	2	-	-
7.6	-NH_2	1	1	-	-
1.45	-CH_3 alanine	10	11	-	-
3.75	C H	6	6	-	-
2.65	N^+-CH_2 carnosine	5	3	-	-
7.0	C-4 (His)	3	4	-	-

*Peak area is shown as square millimeters.

Table 6.I. Quantification of lactate, cholesterol, creatine, taurine in normal(a) and myocardial infarction heart autopsy(b) perchloric acid extracts by ex vivo H-1 NMR spectra shown in Figure 2B. The standard creatine 18 mM solution as reference metabolite was used to measure concentration

Chemical shift (ppm)	Assignment group	Peak area (mm^2)		Concentration (mM)	
		Normal	Myocardial infarction	Normal	Myocardial infarction
3.95	-NCH_2(-PCr)	13	25*	18	63
3.91	-NCH_2(Cr)	11	24	6.1	6.3
3.4	-N+CH_2(taurine)	8	14	16.8	51.9
3.25	-N+CH_3(carnitine)	5	17*	0.20	6.46
3.2	-SCH_2(taurine)	13	34*	67.2	187.5
3.0	-N^+CH_3(PCr+Cr)	17	35*		
2.6	-CH_2-(succinate)	3	1		
2.45	- C H $_2$-(glutamine)	1	1		
2.12	C H $_2$-(glutamine)	1	1		
1.8	Cholesterol	6	3*	0.74	0.10
1.45	-CH_3(alanine)	2	4		
1.33	-CH_3(lactate)	19	3		

*signifies peak assignments with clinical significance.

II. Quantification of metabolites in normal heart (a) and myocardial infarction heart (b) by in vivo H-1 MR spectroscopy is shown in Figure 3B. The standard creatine 18 mM solution as reference metabolite was used to measure concentration

Chemical shift (ppm)	Assignment group	Peak area (mm^2)		Concen - tration (mM)	
		Normal	Myocardial infarction	Normal	Myocardial infarction
1.61	-CH_2-CH_2 (fatty acids)	10	24		
1.83	-CH_3 acetate(cholesterol)	30(11 mm)	35(34 mm)	13.5	30.7*
2.03 and 2.4	C H $_2$(glutamate)	31	26		
2.21	C H $_2$(glutamate)	28	27		

2.63	$=N^{+}CH_2$(alanine)	20	23		
3.02	=NCH(PCr/Cr)	92	117	24	38.1
3.46	$-SCH_2$and$=N^{+}CH_2$(taurine)	57	47		
6.11and6.31	Ribose H^{+}(ATP)	16	15		
6.31					
6.5					
6.52					
6.78	C_2H(tyrosine)				
6.8	C_6H(tyrosine)				
5.5-5.9	-CH=CH-(unsaturated fatty acids)	25	28		

*shows significant peaks with clinical significance.

A

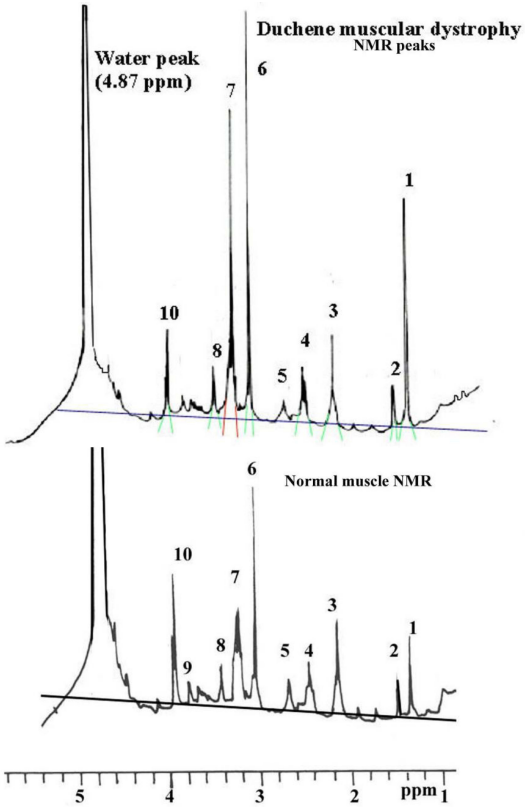

B

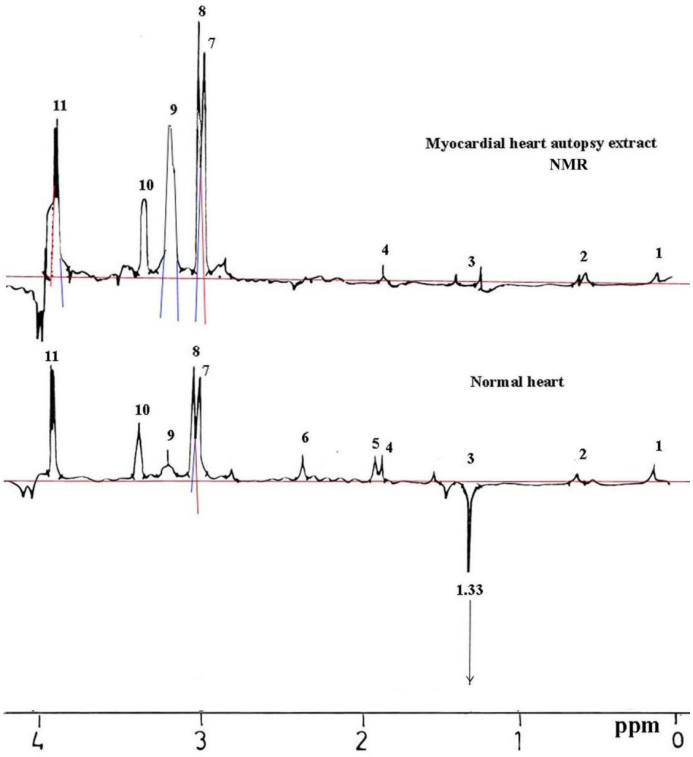

C

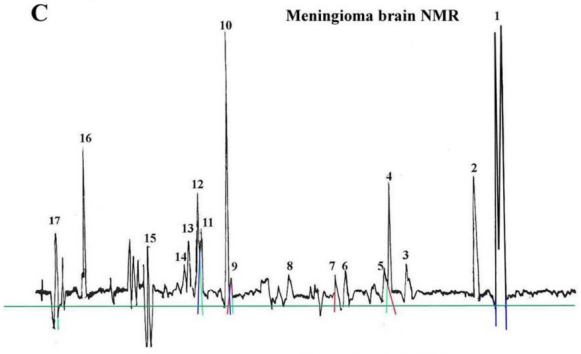

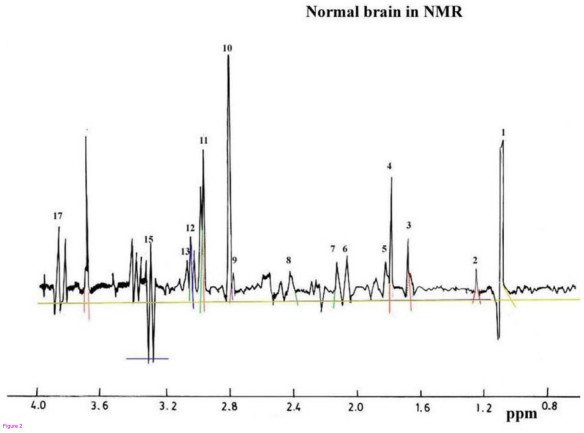

D

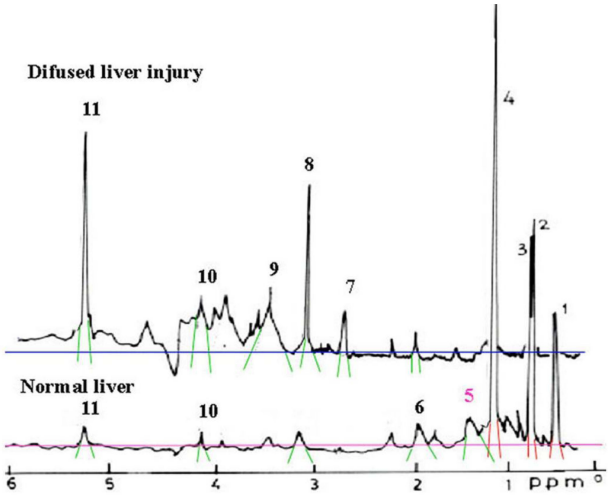

Figure 2. Ex vivo H-1 NMR spectra of normal tissue (a) and diseased tissue (b) are shown for perchloric acid extracts of duchene muscular dystrophy muscle biopsy (Panel A), myocardial infarction heart(Panel B), meningioma brain autopsy(Panel C) and diffused liver injury liver biopsy(Panel D). Spin echo 120 ms against water 4.76 ppm was used. Metabolites were identified as peaks shown in: Panel A: lactate (2,14), glutamate/glutamine (4-6), alanine (3,13), carnosine (7) Panel B: carnosine (7), PCho+glyceroCho (8), taurine (9), PCr/Cr (10), lactate (11), urea (12) Panel C: lactate (1), alanine (2), acetate (3), creatine (4,10) Panel D: cholesterol and fatty acids (1,2,3), lactate (4), alanine (5), glutamine (6), carnosine (7), PCho/glyceroPCho (8), taurine (9), PCr/Cr (10) by selective spin echo pulse sequence.

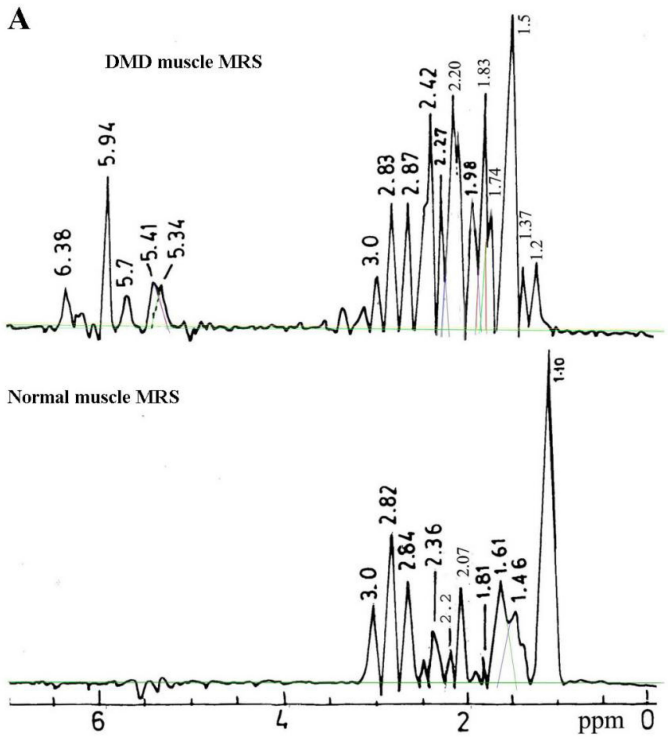

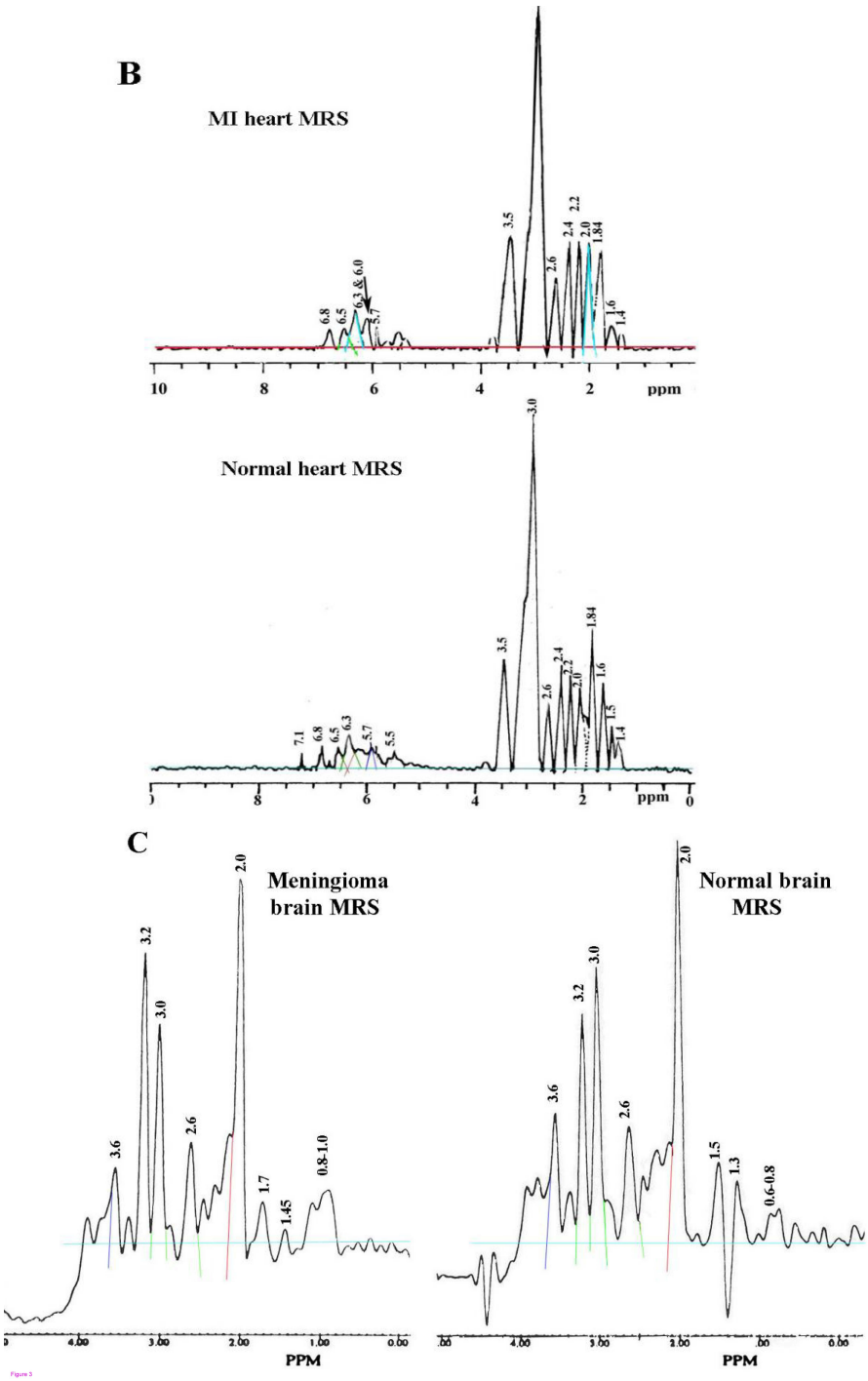

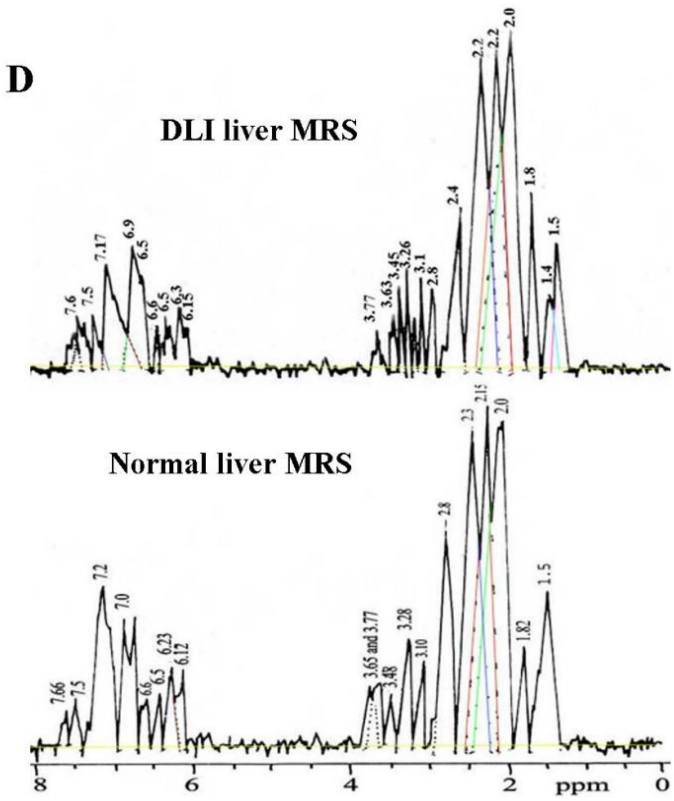

Figure 3. In vivo H-1 MR spectroscopy of normal tissue (a) and diseased tissue (b) are shown for perchloric acid extracts of duchene muscular dystrophy muscle biopsy (Panel A), myocardial infarction heart (Panel B), meningioma brain autopsy (Panel C) and diffused liver injury liver biopsy (Panel D). Localized water suppressed 1331 SPECSUP sequence against water 4.76 ppm as reference remnant peak.

Table 7. I. Quantification of metabolites in normal brain autopsy sample (a) and meningioma brain autopsy perchloric acid extract (b) by ex vivo H-1 NMR spectra as shown in Figure 2C. The standard glutamate 40 mM solution as reference metabolite was used to measure concentration

Peak #	Chemical group	metabolite	Chemical shift(ppm)	Peak area (mm^2)		Concen-tration (mM)	
				Normal	Meningioma	Normal	Meningioma
1	$-CH_3$	Lactate	1.33	18	50	1.44	1.9
2	$-CH_3$	Alanine	1.45	11	65	0.8	2.15
3	$-CH_3$	Acetate	1.87	23	17	0.22	0.11
4	$-CH_3$	NAA	2.02	250*	218	11.4*	9.7
4	$-CH_3$	Creatine	3.0	60*	57	2.61*	2.5
	$-CH_3$	Choline	3.2	30*	38	0.34*	0.44

*shows major peaks with clinical significance.

II. Quantification of fat and amino acid metabolites in normal brain autopsy (a) and meningioma brain autopsy perchloric acid extract(b) by in vivo H-1 MR spectroscopy peaks shown in Figure 3C

Chemical shifts(ppm)	Resonance Assignment	Peak area (mm^2) Normal	Meningioma	Concen-tration (mM) Normal	Meningioma
1.0			32		-
1.2-1.4		16.2	4.2	4.5	1.3
2.02	NAA(-CH_2)	256	178	11.3	9.8
2.2-2.6	Glu/Gln(CH_2)	35	41	2	2.1
2.7	Aspartate(CH_2)	66	63	2.3	2.3
3.0	PCr+Cr(=NCH_3)	102	84	7.4	6.8
3.2	Choline [-$N^+(CH_3)_3$]	76	116	6.6	8.5
3.4	Taurine (SCH_2)	29	31	0.6	0.6
3.6	Myoinositol	41	38	5.3	5.2

*signifies peak assignments with clinical significance.

DISCUSSION

Interpretation of NMR and MRS peaks in tissues pose a problem specially to extract out the metabolite NMR information from *in vivo* clinical NMR spectroscopy [1,2,3,4]. The chapter provides a possible explanation for different T1 and T2 times and degree of NMR visibility of metabolites *ex vivo* and *in vivo* in diseases.

Tissue processing before MR experiments also affects the measurement. Inconsistent water suppression, voxel size, Guassian peaks, Rf coil transmission/reception also affects the in vivo measurement. In our study, selective water saturation spin echo FT method highlighted methyl and methylene groups in different metabolites such as NAA(ABX spin system), lactate/alanine, and methylene groups in choline and glutamine/glutamate as NMR resonance assignments.

Table 8. I. Quantification of lipid, amino acid metabolism in normal liver biopsy (a); and diffused liver injury (b) perchloric acid biopsy extracts by ex vivo NMR spectra shown in Figure 2D. The standard 18 mM creatine solution was used as reference to measure metabolite concentration

Chemical shift	metabolites	Peak area (mm^2)	Diffused Liver	Concentration (mM)	Diffused Liver

(ppm)		Normal	injury	Normal	injury
2.65	alanine (carnosine)	2.5	1.3*	-	-
3.2	PCr+glycerophosphoryl Choline	6	35*	7.2	61.3
3.4	Taurine	5	35*	5.75	23.0
3.9	PCr/Cr	3	34*	0.48	1.06
4.1	Lactate	4	11*	-	-
5.5	Urea	6	73*	-	-

*shows major peaks with clinical significance.

II. Quantification of metabolites in normal liver biopsy (a); and diffused liver injury (b) perchloric acid biopsy extracts by in vivo NMR spectra as shown in Figure 3D. The standard 18 mM creatine solution was used as reference to measure metabolite concentration

Chemical shifts (ppm)	metabolite	Peak area(mm^2) Normal	Diffused liver injury	Concentration (mM) Normal	Diffused liver injury
1.51 and 1.82	$-CH_2$(Fatty acids)	110	98		
2.1-2.32	C H $_2$(glutamate)	430	456	10.08	10.92
2.4-2.5	C H $_2$(glutamate)	186	240	8.6	8.52
2.81	C H $_2$(aspartate)	89	21	6.27	2.7
3.1	$[N^+(CH_3)_3]$Choline	21	12	6.8	3.9
3.28	$[-N^+(CH_3)_3]$Carnitine	32	30		
3.48	$[=N^+(CH_2)]$Carnitine	16	12		
3.63-3.77	- glycerophosphorylcholine	63	40	7.5	5.1
6.1-6.5	$(-CH_2)$Ribose(ATP)	60	42		
6.6-6.7	Tyrosine	50	41		
6.9	Histidine	35	34		
7.1-7.6	Tryptophan	113	88	17.3	12.0

*shows major peaks with clinical significance.

In our study, smaller molecules could be visualized by proton MRS method and *ex vivo* NMR method in perchloric acid tissue extracts. However, *ex vivo* NMR data could be affected by tissue processing method, in particular, macromolecules were poorly NMR-visible [9]. So, comparison of smaller metabolites as fingerprints of disease is highlighted in this study. Moreover, previously smaller metabolites in homogenates were measured without

any loss during tissue processing at temperature controlled condition as fingerprint metabolites for diseased tissue reported [12].

The NMR data comparison with tissue contents and clinical chemistry lab data appear as clinical metabolic-MR correlates in DMD, MI, MB and DLI diseases where T1 and T2 appear as tissue specific and characteristic. The biochemical basis of comparable data may be significant to speculate the metabolite–MR correlates in different diseases are discussed in following discussion.

From NMR spectroscopy standpoint, many methods have been applied to obtain H-1 NMR spectra of living cells by reducing large water signal by H_2O replacement method, water elimination Fourier Transform method, difference of T1 relaxation times between water and other molecules by use of correlation NMR methods [5, 12]. We used selective water saturation FT NMR method at 400 MHz. Spectra showed broad ill defined components from macromolecules in the tissues. To reduce broad components, spin echo FT high resolution spectra were used in which small molecules such as lactate could be detected. Spectral broad components seem to be due to fast relaxing proton fraction and macromolecule protons.

In vitro NMR studies in muscle biopsy sample from DMD used decreased water signal and minor macromolecule signals existing in muscles and reduced complexity, to analyze H-1 NMR spectra of muscle from DMD persons. Elevated *ex vivo* NMR peak amplitudes of lipids, alanine, taurine, and glutamate reflected muscle fibrosis. DMD tissue homogenates and serum chemistry further confirmed the elevated levels of phospholipids, triglycerides in homogenates and serum creatine kinase, SGPT indicating fatty infiltration. Small molecules resonance lines as decreased and narrow resonance lines were partially saturated due to signal tails, making signal intensity necessary for quantification. These lipid signals seem to be originated from the mobile lipids or depot lipids in muscle and not from membrane lipids. In normal muscle, no membrane phospholipids could be observed and only depot lipids could be observed. Mainly they were phospholipids and fatty acids. The high resolution spectra showed also other important metabolites such as phosphocreatine, urea, glutamine, glutamate and alanine. Previously, triglycerol resonance and histidine of anaserine have been reported along with elevated lactate and large peaks of choline, creatine in muscle ischemia [18] (8). In DMD, muscle showed the elevated lipids and carnosine content. In vivo H-1 MR spectroscopy provided the identification of resonances from intracellular metabolites. In vivo MRS peak pattern also suggested fatty infiltration. Earlier depot lipids have been reported in muscle with elevated lactate, choline, creatine in muscle ischemia [19]. Muscle unsaturated/saturated fat ratio and fatty acyl resonances were characterized by peak height ratios of polyunsaturated to carbonyl carbons [12]. Composition and resolution of fatty acyl chains and with quantification of unsaturated-saturated fat ratio in muscle was reported [21](9). The fat metabolism in muscle appears to be altered to synthesize unsaturated fat.

Quantification of metabolites have been approached by the ratio of peak heights of polyunsaturated to carbonyl carbons which showed decreased levels of unsaturated fatty acids in various diseases of muscles as cystic fibrosis, lipoprotein lipase deficiency [20, 22]. These recent studies suggested the same clue for *in vivo* metabolic muscular dystrophy quantitative assessment by NMR if treatment could be started early and diagnosed. It can be concluded that muscles from normal persons show peaks from phosphocreatine/creatine, choline and carnosine as well as fatty acyl chains while DMD affected muscle demonstrated multiple resonances from various fatty acids.

The present study also suggests similar clues for phosphocreatine/creatine and fatty acyl protons in normal and multiple fatty acyl proton NMR resonances. These suggest possible following metabolic reaction catalyzed by creatine kinase:

Phosphocreatine + H^+ + ADP ATP + creatine.

It also supports the elevated levels of serum creatine kinase, reduced phosphocreatine as a result of energy depletion and active oxidative state in DMD muscle. Associated elevation of SGPT in serum and reduced phospholipids in DMD muscle tissue suggested the accumulation of alanine and lactate due to muscle fibrosis and dystrophy. Earlier report suggested similar reduced Pi signal and increased fat (-CH2) signal in dystrophic process (replacement of muscle fibers with fibrous tissue) as reduced phosphocreatine/ATP ratio [13]. Phospholipids generate fatty acids by oxidation (acetyl CoA formation) for mitochondrial ATP generation during relaxation-contraction in muscle. The protons of choline appear to reflect muscle growth status. Earlier different ratio of mono/di unsaturated lipids suggested metastasis [23]. Similarly DMD muscle atrophy and fibrosis can be ascribed as depletion of phosphocreatine, elevated phosphodieaters, fatty acids and fatty infiltration. Muscle fibrosis and energy depletion in Duchene Muscular Dystrophy muscle tissue was common manifestation reflected as elevated *ex vivo* NMR peak amplitudes of lipids, alanine, taurine, and glutamate. The elevated presence of glutamine/glutamate can be speculated due to its rapid generation from NMR visible - ketoglutarate by SGPT and active glutamine/glutamate synthase for energy supply as recently evidenced [14]. Creatine is product of amino acid breakdown and generates phosphocreatine. Taurine facilitates the synaptic connections in ion movement where glutamate is an excitatory amino acid in muscle.

In normal heart spectra, the NMR line widths showed good resolution. In vitro NMR data of human diseased heart autopsy is less known. The spectra showed resonances of α,β,γ - $(CH_2)_n$- and terminal methyl protons visible in myocardial infarct heart autopsy perchloric extracts indicated energy metabolic depletion and fatty infiltration. Other elevated major metabolites were lactate, Cr+PCr and diminished taurine with unaletered fatty acids or lipids. In normal heart, taurine was present in large quantities in cardiac tissue and carnitine was not

as abundant because myocardium has fatty acyl carnitine. Considering number of protons contributing to each resonance, relative intensities of taurine and carnitine peaks were consistent with previously reported values [24]. Myocardial glycosides were seen in spectra and they were thought to be distributed in several pools without different metabolic turnover rates as well as biochemical characteristics. In spectra, several peaks were observed from metabolically mobilizable myocardial glycerides and free fatty acids but not from rapid turnover glycerides. Moreover, glycerides were not NMR visible in heart extracts. The reason may be that multiple glyceride pools based upon metabolic turnover, possess different physical characteristics and large accumulated amount in heart were not visible. Although, biochemical assays showed elevated serum triglycerides and suggested possibility of slow and high rate turnover of myocardial triglycerides. Distinct phospholipids and triglycerides after fasting were identified and quantitated by NMR spectra but fatty acid chains remained unchanged [25]. It showed two myotriglycerides pools: slow rate turnover and high rate turnover. In present study, no accumulation of lactate or lesser extent was observed with unaltered taurine, carnitine in myocardial infarction heart NMR[26]. It may be attributed to the fact that lactate easily traverses across cell membranes or would have washed away during perchloric acid extraction. Thus H-1 NMR spectra of cardiac muscle can be used for the diagnosis of cardiac disorders.

The effect of myocardial lipid deposition on the signal peaks from alanine, glutamate and aspartate can be attributed to the fact that alanine is a product of pyruvate after glycolysis and diseased heart tissue reduces its ability to oxidise lactate when returned to oxidative metabolism. Increased succinate can be attributed to inoperative citrate to ketoglutarate in tricarboxylic acid cycle [27]. The α-Ketoglutarate production comes from alanine transamination (alanine transferase) which is the primary source of succinate. Thus alanine and ketoglutarate maintain a balance. The α-Ketoglutarate generates less glutamate by glutamate dehydrogenase reaction, showing glutamate fall observed in spectra. Thus ketoglutarate rapidly gets converted to succinate and less to glutamate. Simultaneously, oxaloacetate gets converted to malate by increased $NADH/NAD^+$ ratio leaving low oxaloacetate content. So malate, alanine and succinate metabolites showed a rise in myocardial muscle due to continuous consumption of glutamate and aspartate in alanine aminotransferase reactions (glutamate uptake and alanine release) and aspartate aminotransferase reactions (aspartate oxaloacetate and malate). It is to be noted that alanine and succinate accumulation in energy depleted heart muscle was accompanied by release of lactate. Lactate and alanine are known to pass through the heart cell membranes radily while succinate kinetics is not known. Succinate appearance in extracellular space may be due to membrane damage or its enhanced synthesis. The ability of alanine and succinate to diffuse into myocardium indicates value of these compounds as markers of cardiac oxidative defect. So, release of metbolites seems to be lactate > alanine > succinate > creatine. However, MI

heart homogenates and sera chemistry also indicated elevated triglycerides, cholesterol and lactate in homogenates and serum triglycerides, creatine kinase-MB as previously reported [28].

Proton localized in vivo MR spectroscopy showed elevated cholesterol, alanine, glutamate, aspartate peaks and suggested more energy demand as metabolite characteristic of heart and suggested the potential of H-1 spectroscopy for providing insights into biochemical metabolic status of heart wall. In cardiac muscle metabolic spectroscopy, shimming and water referencing were done by surface coil position under chest. The heart motion effects and shape of water peak problems were reduced by shimming. Homogenous water peak was obtained. Resonances from PCr/Cr and taurine were characteristically unchanged but additional saturated fatty acid resonances were observed in the aliphatic region 1.6 – 2.55 ppm and 5.7 – 5.95 ppm due to –CH=CH- protons which is related with decreased unsaturated/saturated fatty acid ratio in the tissue [14, 29]. Our data corroborates with these metabolites except lactate [29]. Other reports on ^{31}P-MR spectroscopy using rotating frame technique, ISIS also indicates additional saturated fatty acids and lactate levels in myocardial infarction and phospholipids characterization [30, 31]. In present study, we did not observe lactate peak. Elevated creatine phosphokinase-MB suggested a scientific explanation to interpret the reason of disease and perhaps may be helpful in therapeutic monitoring. Higher glutamate appearance in MR spectra was also supported because of its protective action [32]. Moreover, myocardial infarction and lipid metabolites have been reported where distinct metabolites ratio and quantification was attempted [33]. It may be concluded that energy metabolic depletion and fatty infiltration in myocardial infarcted heart autopsy were possibly manifested as elevated *ex vivo* NMR peaks of elevated lactate, diminished taurine, Cr+PCr and unaltered fatty acids or lipids in MI heart homogenates. *In vivo* MRS exhibited elevated cholesterol, alanine, glutamate, aspartate due to more energy requirement in tissue.

The ex vivo NMR spectroscopy of meningioma brain autopsy samples exhibited several metabolites by chemical shift peak positions for lactate, glutamine, glutamate and choline. Applicability of H-1 NMR for characterization of distinct metabolites in normal and meningioma tissue has been established based on the localized differences at different sections of brain sites. Our study shows that lactate and other metabolites in brain autopsy samples of meningioma brain have elevated levels as compared to normal brain spectra. In present study, meningioma brain spectra showed poor resonance peaks of low N-acetylaspartate, glutamate, glutamine, pyruvate, acetoacetate, phosphocreatine/creatine but showed major resonances from lactate, choline and alanine with aspartate and taurine. The absence of glutamine/glutamate in meningioma may be attributed to lack of enzyme system (glutamate synthase/aspartate transaminase) perhaps leading to taurine accumulation. Low phosphocreatine in meningioma than the normal brain tissue could be attributed to lower supply of glycine and ornithine to remove ammonia which leads to hyperammonemia and

decreased glutamate available [34]. The meningioma spectra did not show enhanced signals of choline containing compounds. Moreover, the lipids, lactate and glucose contents in meningioma tumors could not be characterized further.

The H-1 localized spectroscopic observations suggested NAA, creatine and choline show up as distinct assignments by both NMR and localized MR spectroscopy. Neuronal changes in meningioma brain appear associated with elevated ex vivo NMR peaks of lactate, choline and alanine but depleted peaks of NAA, glutamate/glutamine, pyruvate, acetoacetate. Previous study reported *in vivo* volume localized ^{1}H spectroscopy suggested intensity of N-acetylaspartate, and creatine in meningioma less than normal tissue intensities but elevated choline and lactate resonance similar to our observations [34-37]). Water suppressed proton spectroscopy still is a new method for analyzing fat content of brain tissue because of good resolution of various protons in fatty acyl chains and area analysis under peak to visualize unsaturated/saturated fat ratio in the tissue. Better picture of disease was reported by energy metabolites ATP, ADP and AMP along with inorganic Pi and sugar phosphates by ^{13}C NMR and ^{31}P NMR indicating metabolites mainly participate in energy regulation [38]. Rise of Pi stimulates the glycolysis and lactate production, causing acidosis. Both the PCr and ATP depleted and Pi accumulates while ADP is lost via conversion to AMP, inosine phosphate (IMP), adenine and ultimately hypoxanthine and urates. Immobilized ion pump Na^{+}/K^{+} causes irreversible membrane structural damage accompanied by elevated glutamate which is NMR visible. The above sequence of metabolite generation occurs in brain during diseased state. Brain phosphomonoeasters as phosphotydylethanolamine, plasmalogens in white matter and myelin, are mainly synthesized by ethanolamine kinase and desaturase during myelinogenesis. Thus PME/ATP and PME/PDE ratio seem useful ^{31}P NMR tools. Glycerophosphocholine and glyceroethannolamine are phosphodiesters and are synthesized during myelination by ethanolamine phosphotransferase. NAA provides anion balance in brain, acetyl group transport, contribution of acetyl groups for fatty acid synthesis, regulation of myelin synthesis, acetyl CoA and biogenic amine generation in brain (NAA-glutamate). Taurine facitates further brain neurone synaptic connection in developing neuronal tissue and further controls ion movement, magnesium homeostasis and maintains structural integrity of brain cell membranes because of its ability to modulate calcium homeostasis. Glutamate is excitatory amino acid neurotransmitter and plays a part in trnasamination. In meningioma, N-acetylaspartate, creatine decreased while choline and taurine accumulated. Neuronal changes in meningioma brain were associated with elevated *ex vivo* NMR peaks of lactate and alanine but depleted peaks of pyruvate, acetoacetate, choline. *In vivo* MRS exhibited elevated N-acetyl aspartate (NAA) and choline peaks.

In water saturated spin-echo FT, in vitro NMR spectroscopy of normal liver biopsy evidenced histidine, tryptophan, choline, glutamate/glutamine. Water and macromolecules signals were sufficiently suppressed. Spin echo based H-1 NMR spectra were largely reported

on alternatively adding and substracting modulated spectra obtained from CPMG and Hann spin echo experiments [39]. Still reports are not conclusive on liver metabolic information using in vitro NMR methods. Consequently, human liver in vivo H-1 NMR is not currently acceptable in clinical set up. In our study, normal liver NMR spectra showed fatty acyl $–CH_2$-protons, glutamate/glutamine, choline, carnitine, glycerophosphoryl choline, aromatic amino acids. Diffused liver injury liver biopsy demonstrated a depletion of unsaturated fatty acid, glutamate/glutamine, lactate and dynamic lipids. However, mobile lipids could not be discriminated even by exploiting metabolite T2 differences. For other metabolites such as glycerophosphoryl choline and depleted glutamate/fatty acid pool peaks were NMR visible. These NMR peaks were associated with elevated levels of ALT and AST transaminase, cholesterol, bilirubin and alkaline phosphatase in serum. This may be explained on the basis of parenchymal cells capacity decreased for clearing glycerophosphoryl compounds and active deposits of fats which is generally one of the precipitating factors of “fatty liver” condition supported by histology findings [40]. As a result of this liver condition, liver intracellular energy flux presumably diverts towards more ATP generation which needs acetyl CoA, a regulatory central metabolite. It can be explained originated either from β oxidation of fatty acid or originated from glutamate by transamination. Eventually, it leads to depleted glutamate and fatty acid pools and cholesterol, serum glutamate transaminase and phospholipids. In general, in vitro H-1 NMR spectral peaks allowed identification of well defined intracellular metabolites characteristic of normal liver. Although pathophysiological mechanisms of diffused liver injury are poorly defined, resonance peak metabolite quantification by spectroscopy provides noninvasive insight of metabolite identification and possible biochemical characterization. Composition of lipids and fatty acyl chain chemicals were resolved and quantified as unsaturated-saturated fat ratio in liver to infer the cause of diffused liver injury [41]. The fatty metabolites in liver associated with liver injury have been attributed to higher concentration of cholesterol, triglyceride and free fatty acids, glutamate, amino acids and phospholipids in circulation, which leads to accumulation of saturated lipids, which may be assessed by H-1 MR spectroscopy. Earlier quantification of metabolites has been approached by peak height ratio of polyunsaturated fatty acid and carbonyl proton peaks which were decreased in various diseases such as alcohol liver disease, hepatitis and transplantation graft viability assessment [42]. Liver has parenchymal and nonparenchymal cells responsible for intracellular metabolism. Parenchymal cells regulate glycolysis, tricrboxylic acid cycle, and energy storage in the form of fatty acids [43]. Mainly pyruvate oxidation, lactate accumulation and higher consumption of glutamate/glutamine seem to be evident in diffused liver injury[44]. In mitochondria, ATP production by NADH oxidation and oxidative phosphorylation is needed for gluconeogenesis, lipogenesis[45]. In liver injury, ATP supply becomes paralyzed leading to depletion of phosphocreatine and alkalosis. Fatty infiltration and lactate accumulation and saturated lipids in diffused liver injury (DLI) liver

tissue were manifested as elevated *ex vivo* NMR lactate, lipid peaks [46, 47]. It was concluded that H-1 NMR spectroscopy can identify lactate, glutamate/glutamine, glucose, creatine, ATP, aspartate, fatty acids and glucose. *In vivo* MRS showed depleted amino acids due to fatty infiltration. Thus both biochemical and MR findings show lactate accumulation, depleted glutamate, unsaturated fatty acids, glucose and phosphocreatine.

Limitations of present study: We could not get clue for mechanism of disease, turn over or biosynthesis because of NMR analysis only visualized the elevated metabolites in tissue. Combining NMR metabolite data with metabolites in tissue homogenate contents and sera appears to speculate many systematic events and new biochemical definition of fatty infiltration, neuronal dysfunction and energy depletion. In near future, continuing efforts of high resolution NMR combined with localized diffusion, perfusion, functional MR imaging methods may be ideal for biochemical characterization of diseases. In future, better computer peak analysis and MRS with MRI techniques presumably will provide on-line MRS peaks and localized metabolite composition with more accuracy.

Limitations of present study: We could not get clue for mechanism of disease, turn over or biosynthesis because of NMR analysis only visualized the elevated metabolites in tissue. Combining NMR metabolite data with metabolites in tissue homogenate contents and sera appears to speculate many systematic events and new biochemical definition of fatty infiltration, neuronal dysfunction and energy depletion. In near future, continuing efforts of high resolution NMR combined with localized diffusion, perfusion, functional MR imaging methods may be ideal for biochemical characterization of diseases. In future, better computer peak analysis and MRS with MRI techniques presumably will provide on-line MRS peaks and localized metabolite composition with more accuracy.

CONCLUSION

Ex vivo and *in vivo* NMR spectral peak observations in different diseases can support the reliability of clinical applications using *in vivo* localized H-1 MR spectroscopy peaks to determine the biochemical cause of disease. In future, better computer peak analysis and MRS techniques presumably will provide on-line MRS peaks with more accuracy. However, peak identification, peak analysis, quantitation of metabolites from *ex vivo* NMR and *in vivo* MRS data is presently, remains a big challenge.

ACKNOWLEDGEMENTS

I acknowledge my Ph.D supervisors for the suggestions and corrections made by Drs. Jose Katz, MD, Ph.D. and Paul Cannon, MD both at Radiology and Medicine departments, College of Physicians and Surgeons, Columbia University, New York.

APPENDIX I:

STRATEGY OF METABOLITE QUANTITATION BY MR SPECTROSCOPY

For in vitro and in vivo NMR spectroscopy, there is imperative need of reliable peak processing to measure metabolites due to broad and inhomogeneous overlapped peak shapes. Many methods based upon NMR signal time domain fitting to specific model functions are available like LPSVD, HSVD, MEM using Lorentzian or Gaussian line shapes. However, deviated line shapes of spectra cannot be corrected. We used the following methods for metabolites.

1. For N-acetyl aspartate, creatine/phosphocreatine and choline: Using fully relaxed water signals as an internal standard, the average metabolite concentrations in volume of interest (VOI) was calculated as:

Concn of NAA = Concn of water (NAA peak area x 2)/ (water peak area x 3)

Concn of PCr/Cr = Concn of water (PCr.Cr peak area x 2)/(water peak area x 3)

Concn of Choline = Concn of water (Cho peak area x 2)/(water peak area x 9)

Peak area denoted signal peak correlated for both T1 and T2 relaxation. Water signal is related with peak area as:

Area under peak = $S\ (1- e^{-TR/T1})$, where S is area under peak to a given TR repetition time and S is signal at $TR = \infty$

Area under peak = $S_o\ (e^{-TE/T2})$ where S_o is area under peak to a given TE echo time and S_o is signal at TE = 0 as described earlier [1].

Internal water was used as standard to calculate metabolites by proton unsuppressed MR spectra. Other less visible metabolites can be compared with water peak area at tissue water concentration 55 M.

2. For Phospholipids, inorganic phosphorus and cholesterol: By comparing digital integration of peaks with that of internal standard, concn can be measured:

$W_u = W_s \times S_f (N_s. M_u. I_u)/(N_u. M_s. T_s)$, where W_u and W_s are weights of unknown and standard solutions, N_u and N_s are active nuclei number, M_u and M_s are molecular weights, Iu and Is are signal integrals of unknown and standard solutions, S_f is saturation factor. The molecular weights of standards were: cholesterol(380), phospholipids(750), P_i(95) as described earlier [2].

3. For glutamate, N-acetyl aspartate, glutamine, aspartate: Addition reference signal resonance with same lineshape was introduced which depends upon spin-spin relaxation time (T2). The signal represents FID having pure Lorentzian lines.

$S(t) = Vj \exp[i . t] \exp^{(-t/T2j)}$ where $1/T_2j = [1/ T_2j – 1/T2r + 1/T]$ where T_2j is spin-spin relaxation, r is spatial dependency, is frequency of j^{th} line.

The concentration $I_{EK} = (A_k/A_u)(C_u/C_k)(3/N_k)$ where I_{EK} is effective signal intensity of unknown compound, A_k and A_u are amplitudes of known and unknown compounds, C_k and C_u are concentrations. N_k is number of protons contributing of known components [3].

1. Christiansen P, Henriksen O, Stubgaard M, Gid P, Larsson HBW. In vivo quantitation ofbrain metabolites by H1 NMRS using water as an internal standards. Magnetic Resonance Imaging.1993,11:107-118.
2. Mariner DM. High resolution NMR spectroscopy of cerebral white matter in multiple sclerosis. Magnetic Resonance in Medicine 1990,13:343-357.
3. Van Dijk JE, Mehlkopf AF, Ormondt DV, Bovee WMMJ. Determination of concentrations by time domain fitting of proton NMR echo signals using prior knowledge. Magnetic Resonance in Medicine 1992,27:76-96.

REFERENCES

[1] Helms G. A precise and user-independent quantification technique for regional comparison of single volume proton MR spectroscopy of the human brain. *NMR Biomed.* 2000 Nov;13(7):398-406.

[2] Keevil SF, Barbiroli B, Brooks JC, Cady EB Absolute metabolite quantification by in vivo NMR spectroscopy: II A multicentre trial of protocols for in vivo localized proton studies of human brain. *Magn Reson Imaging* .1998:16(9):1093-1106.

[3] Li BS, Babb JS, Soher BJ, Maudsley AA, Gonen O. Reproducibility of 3D proton spectroscopy in the human brain. *Magn Reson Med*. 2002 Mar;47(3):439-46.

[4] De Beer R, Barbiroli B, Gobbi G, Knijn A, Kugel H, Langenberger KW, Tkac I, Absolute metabolite quantification by in vivo NMR spectroscopy: III. Multicentre 1H MRS of the human brain addressed by one and the same data-analysis protocol. *Magn. Reson Imaging*. 1998 Nov;16(9):1107-11.

[5] Ross B, Michaelis T. Clinical applications of magnetic resonance spectroscopy. Magnetic Resonance Quarterly. 1994; 10(4): 191-247.

[6] Fan G, Sun B, Wu Z, Guo Q, Guo Y. In vivo single-voxel proton MR spectroscopy in the differentiation of high-grade gliomas and solitary metastases. *Clin. Radiol*. 2004 Jan;59(1):77-85.

[7] Matson GB, Weiner MW. Spectroscopy: In *Magnetic Resonance Imaging*. Ed. Stark DD and Bradley WG, Mosby year book St. Louis, Missouri (1992)438-478.

[8] Binesh N, Yue K, Fairbanks L, Thomas MA.Reproducibility of localized 2D correlated MR spectroscopy. *Magn. Reson. Med.* 2002;48(6):942-8.

[9] Lindon JC, Nicholson JK, Holmes E, Everett JR. Metabonomics: Metabolic processes studied by NMR spectroscopy of biofluids. *Concepts in Magnetic Resonance Part A*. 2000, 12(5):289 – 320.

[10] Boehringer Mannheim GmbH Diagnostica Automated Analysis:1. Instruction manual to clinical chemistry (2001).

[11] Sharma U, Atri S, Sharma MC, Sarkar C, Jagannathan NR. Skeletal muscle metabolism in Duchenne muscular dystrophy (DMD): an in-vitro proton NMR spectroscopy study. *Magn Reson Imaging*. 2003 Feb;21(2):145-53.

[12] Gupta RK, Roy R, Dev R, Husain M et al. Finger printing of Mycobacterium tuberculosis in patients with intracranial tuberculomas by using in vivo, ex vivo, and in vitro magnetic resonance spectroscopy. *Magn. Reson. Med.* 1996 Dec;36(6):829-33.

[13] Price WS. Water signal suppression in NMR spectroscopy. *Annual Report NMR Spectroscopy*, 1999, 38:290-349.

[14] Sprott H, Rzanny R, Reichenbach JR, Kaiser WA, Hein G, Stein G. ^{31}P magnetic resonance spectroscopy in fibromyalgic muscle. *Rheumatology* (Oxford). 2000 Oct;39(10):1121-5.

[15] Pohost GM, Meduri A, Razmi RM, Rathi VK, Doyle M. Cardiac MR spectroscopy in the new millennium. *Rays.* 2001 Jan-Mar;26(1):93-107.Review.

[16] Abe Y, Yamashita Y, Tang Y, Namimoto T, Takahashi M.Calculation of T2 relaxation time from ultrafast single shot sequences for differentiation of liver tumors: comparison of echo-planar, HASTE, and spin-echo sequences. *Radiat Med*. 2000;18(1):7-14.

[17] Tarasow E, Panasiuk A, Siergiejczyk L, Orzechowska-Bobkiewicz A, Lewszuk A, Walecki J, Prokopowicz D. MR and 1H MR spectroscopy of the brain in patients with liver cirrhosis and early stages of hepatic encephalopathy. *Hepatogastroenterology*. 2003;50(54):2149-53.

[18] Deoni SC, Williams SC, Jezzard P, Suckling J, Murphy DG, Jones DK. Standardized structural magnetic resonance imaging in multicentre studies using quantitative T1 and T2 imaging at 1.5 T. *Neuroimage*. 2008;40(2):662-71.

[19] Arus C, Barany M, Westler WM, Markley JL. 1H NMR of intact muscle at 11 T. *FEBS Letters* 165, 231. 1984.

[20] Schick F, Eismann B, Jung WI, Bongers H, Bunse M, Lutz O.Comparison of localized proton NMR signals of skeletal muscle and fat tissue in vivo: two lipid compartments in muscle tissue. *Magn. Reson. Med.* 1993 Feb;29(2):158-67.

[21] Narayana PA, Slopis JM, Jackson EF, Jankovic J, Butler IJ Proton Magnetic Resonance spectroscopic studies of hyperpolarized muscle. Effect of botulinum toxin treatment. *Investigative Radiol 1*991,26(1) 58-64.

[22] Bertocci LA, Mize CE. The use of nuclear magnetic resonance to study muscle metabolism in very low birth weight infants. *Seminars Pediatrics* 1990,14(3):231-7.

[23] Narayana PA, Jackson EF, Hazle EF, Fotedar LK et al. In vivo localized 1H NMR spectroscopic studies of human gastronemius muscles. *Magn. Reson. Med*. 1989,12(2) 259-260.

[24] Buckman DK, Chapkin RS, Erickson KL. Modulation of mouse mammary tumor growth and linoleate enhanced metastasis by oleate. *J. Nutr*. 1990;120(2):148-57.

[25] Pisarenko OI; Mechanisms of myocardial protection by amino acids: facts and hypotheses; *Clin. Exp. Pharmacol Physiol*. 1996; 23(8):627-33.

[26] Booth RF. Lipid characterization in an animal model of atherosclerosis using NMR spectroscopy and NMR imaging. *NMR in Biomedicine*.1990,3(2) 95-100.

[27] Trouard TP, Altbach MI, Hunter GC, Eskelson CD, Gmitro AF. MRI and NMR spectroscopy of the lipids of atherosclerotic plaque in rabbits and humans. *Magn. Reson. Med.* 1997;38(1):19-26.

[28] Wischmeyer PE, Jayakar D, Williams U, Singleton KD, Riehm J, Bacha EA, Jeevanandam V, Christians U, Serkova N. Single dose of glutamine enhances myocardial tissue metabolism, glutathione content, and improves myocardial function after ischemia-reperfusion injury. *JPEN J. Parenter Enteral Nutr*. 2003;27(6):396-403.

[29] Spindler M, Saupe KW, Tian R, Ahmed S, Matlib MA, Ingwall JS. Altered creatine kinase enzyme kinetics in diabetic cardiomyopathy. A(31)P NMR magnetization transfer study of the intact beating rat heart. *J. Mol. Cell Cardiol*. 1999;31(12):2175-89.

[30] Mihara F, Kuwabara Y, Yoshida T, Yoshiura T, Sasaki M, Masuda K,Matsushima T, Fukui M. Correlation between proton magnetic resonance spectroscopic lactate measurements and vascular reactivity in chronic occlusive cerebrovascular disease: a comparison with positron emission tomography. *Magn. Reson. Imaging*. 2000;18(9):1167-74.

[31] Houkins K, Kwee IL, Nakada T. Persistent high lactate levels as sensitive MR spectroscopy indicator of completed infarction. J Neurosurgery.1990,72(5) 763-766.

[32] Sabrina M, Ronen Hadassa D. Application of 13C NMR to characterization of phospholipids metabolism in cells. *Magn. Reson. Med* 1992,25:384-389.

[33] Choi CG, Yoo HW. Localized proton MR spectroscopy in urea cycle defect. *Am. J. Neuroradiol.* 2001,22:834-837.

[34] Evanochko WT. NMR spectroscopic assessment of altered myocardial lipid metabolism. *Investigative Radiology*. 1989, 24(12) 973-975.

[35] De Graaf AA, Dentz NE, Bosman DK, et al. The use of in vivo proton NMR to study the effects of hyperammonemia in the rat cerebral cortex. *NMR in Biomedicine*. 1991,4(1) 31-37.

[36] 34.Sibson NR, Mason GF, Shen J, Cline GW, Herskovits AZ, Wall JE, Behar KL, Rothman DL, Shulman RG. In vivo (13)C NMR measurement of neurotransmitter glutamate cycling, anaplerosis and TCA cycle flux in rat brain during. *J. Neurochem*. 2001 Feb;76(4):975-89.

[37] Harting I, Hartmann M, Bonsanto MM, Sommer C, Sartor K. Characterization of necrotic meningioma using diffusion MRI, perfusion MRI, and MR spectroscopy: case report and review of the literature. *Neuroradiology*. 2004;46(3):189-93.

[38] Cho YD, Choi GH, Lee SP, Kim JK. Characterization of necrotic meningioma using diffusion MRI, perfusion MRI, and MR spectroscopy: case report and review of the literature. *Neuroradiology*. 2004;46(3):189-93.

[39] Opstad KS, Provencher SW, Bell BA, Griffiths JR, Howe FA. Detection of elevated glutathione in meningiomas by quantitative in vivo 1H MRS. *Magn. Reson. Med*. 2003 Apr;49(4):632-637.

[40] Abe Y, Yamashita Y, Tang Y, Namimoto T, Takahashi M. Calculation of T2 relaxation time from ultrafast single shot sequences for differentiation of liver tumors: comparison of echo-planar, HASTE, and spin-echo sequences. *Radiat Med*. 2000;18(1):7-14.

[41] Das TP, Saha AK. Mathematical analysis of the Hahn spin echo experiment. *Physics review*. 1954,93(4):749-756.

[42] Moser E, Holzmuller P, Gomiscik G. Liver tissue characterization by in vivo NMR. Tissue handling and biological variation. *Magn. Reson. Med*. 1992,24(2): 213-220.

[43] Mitchell DG, Stark DD, Glastad K. *Liver in Magnetic Resonance Imaging*. Ed. Stark DD and Bradley WG.Mosby Year Book, St Louis, Missouri, 1994:167-210.

[44] Anzus PW, Dixon RM, Rajgopalan B et al. A study of patients with alcoholic liver disease by 31P NMR spectroscopy. *Clinical Science*. 1990,78:33.

[45] Holzmuller P, Moser E, Reckendorfer , Burgmann H et al. Proton spin lattice relaxation time as liver transplantation graft viability parameter. *Magn Reson Imaging*. 1993,11:229-239.

[46] Tarasow E, Panasiuk A, Siergiejczyk L, Orzechowska-Bobkiewicz A, Lewszuk A, Walecki J, Prokopowicz D. MR and 1H MR spectroscopy of the brain in patients with liver cirrhosis and early stages of hepatic encephalopathy. *Hepatogastroenterology*. 2003;50(54):2149-53.

[47] Tarasow E, Panasiuk A, Siergiejczyk L, Orzechowska-Bobkiewicz A, Lewszuk A, Walecki J, Prokopowicz D.MR proton spectroscopy in liver examinations of healthy individuals in vivo. *Med. Sci. Monit*. 2002;8(2):36-40.

[48] Garbow JR, Lin X, Sakata N, Chen Z, Koh D, Schonfeld G. In vivo MRS measurement of liver lipid levels in mice. *J. Lipid Res*. 2004,45(7):1364-71.

[49] Nardo B, Caraceni P, Pasini P, Domenicali M, Catena F, Cavallari G, Santoni B, Maiolini E, Grattagliano I, Vendemiale G, Trevisani F, Roda A, Bernardi M, Cavallari A. Increased generation of reactive oxygen species in isolated rat fatty liver during postischemic reoxygenation. *Transplantation.* 2001;71(12):1816-20.